*Journal of Thermal Analysis, Vol. 38 (1992) 2529-2548*

*Special Review*

# HIGH-PRESSURE DIFFERENTIAL THERMAL ANALYSIS (HP-DTA)
# II. Dehydroxylation reactions at elevated pressures in phyllosilicates

*S. Guggenheim and A. F. Koster van Groos*

DEPARTMENT OF GEOLOGICAL SCIENCES, UNIVERSITY OF ILLINOIS AT CHICAGO
CHICAGO, ILLINOIS 60680*

(Received March 4, 1992)

High-pressure differential thermal analysis results are used to describe dehydroxylation reactions for the clay materials of kaolinite, Na-rich montmorillonite, and K-, Ca-, and Mg-exchanged montmorillonite. Sealed capsules may be used to contain fluids and it is possible to evaluate the role of $H_2O$ in these reactions. Furthermore, structural information is used with DTA data to develop atomistic models to understand these processes.

**Keywords:** dehydration reactions, high-pressure differential thermal analysis, kaolinite, montmorillonite

## Introduction

Part I of this review [1] illustrated how HP-DTA may be used to understand the effect of pressure on the dehydration reactions in several clay and clay-like

* Correspondence to: Stephen Guggenheim / A. F. Koster van Groos
Dept. of Geological Sciences, m/c 186
University of Illinois at Chicago
P.O.Box 4348
Chicago, Illinois 60680 USA

*John Wiley & Sons, Limited, Chichester*
*Akadémiai Kiadó, Budapest*

materials. It was shown that when pressure is added as a variable, a pressure-temperature grid may be used to determine phase relationships, in addition to the determination of enthalpy. The HP-DTA system described also allows the use of closed capsules, which enable experiments with $P_{H_2O} = P_{total}$.

This paper expands the review to include dehydroxylation reactions of kaolinite, Na-rich montmorillonite, and K-, Ca-, and Mg-exchanged montmorillonite. Refer to Part I for an introduction to the HP-DTA experimental method and to the structure of these materials. Like Part I, emphasis is placed on integrating data from DTA experiments and structural data from other methodologies to understand the processes involved. Portions of this review are from Koster van Groos and Guggenheim [2].

*Sample preparation and characterization*

The starting materials used in the DTA studies described below are a kaolinite from the Coss Hedger Pit, near Sandersville, Washington County, Georgia, and a Na montmorillonite from the Newcastle Formation of Crook County, Wyoming (Clay Mineral Society Source Clays KGa-1 and SWy-1 respectively, see [3]). K, Ca and Mg exchanges were made for the Na-rich SWy-1 montmorillonite; these samples are referred to as KSWy-1, CaSWy-1, and MgSWy-1, respectively. See Part I for a description of the preparation of the starting materials and details of the procedures for exchange. Part I provides also chemical data and mineralogical information for these samples. The chemistry of KGa-1 is given in Table 1.

**Table 1** Chemical analyses of kaolinite KGa-1

| | KGa-1[1] |
|---|---|
| $SiO_2$ | 44.6 |
| $TiO_2$ | 1.44 |
| $Al_2O_3$ | 38.8 |
| $Fe_2O_3$ | n.a. |
| FeO | .05 |
| MgO | .02 |
| CaO | .02 |
| $Na_2O$ | .07 |
| $K_2O$ | 0.04 |

n.a. not analyzed.

[1]Bulk sample analyses averaged from two analyses each as given by [3].

## Dehydroxylation reactions of dioctahedral aluminous phases

Hydroxyl groups in these structures are strongly bonded, and high temperatures are necessary for their removal. The temperature of dehydroxylation is determined by the nature of the hydroxylated phase and thus, by its structure and chemistry. As was discussed in Part I, the kaolinite structure (1:1 type layer) differs considerably from montmorillonite (2:1 type layer) in that most of the hydroxyl groups in kaolinite are located in the plane adjacent to the interlayer, whereas in montmorillonite they are within the 2:1 layer. This may be the reason for the lower dehydroxylation temperature of kaolinite (~600°C at 1 bar) than for montmorillonite (~700°C at 1 bar), although both phases are aluminous dioctahedral varieties.

In general terms, however, the (metastable) phase relationships of kaolinite and montmorillonite show similar geometries (see below). Thus, the delocalization mechanism of the hydrogen must be sufficiently similar in these phases to dominate the phase relations. More specifically, in the kaolinite-$H_2O$ and montmorillonite-$H_2O$ systems, the nature of dehydroxylation involves a topotactic transformation, with the formation of metakaolinite and montmorillonite dehydroxylate, respectively.

### *Kaolinite*

#### HP-DTA data

The results of a series of HP-DTA runs with kaolinite ($Al_2Si_2O_5(OH)_4$), using open and closed capsules, are shown in Fig. 1 [4]. In the open-capsule runs, the peak shape at pressures <45 bars differs from the higher pressure experiments, which suggests that the dehydroxylation mechanism is affected by pressure. For example, at 1 bar the peak-width for the kaolinite dehydroxylation reaction is ~100°C compared to less than 50°C at >30 bars and ~20°C at 1240 bars. The narrow peaks at high pressures indicate that the increase in pressure either affects the dehydroxylation process by making the OH groups more alike energetically, resulting in a uniform dehydroxylation event, or that a different type of reaction occurs. This effect may be augmented by an increase in the rate of the dehydroxylation reaction caused by the increase in temperature. The data also show that at pressures to ~45 bars the dehydroxylation reaction has a strong positive slope. The run products were composed of a soft, fine, white powder, identified as metakaolinite by X-ray powder diffraction (XRD), where metakaolinite is an ill-defined kaolinite-like structure with perhaps some hydroxyl remaining [5, 6]. Above 45 bars, pressure has little effect on the reaction temperature. In these experiments the run products were dominated by a hard, amorphous phase assemblage. In contrast, in closed-capsule runs, where $P_{H_2O} = P_{total}$, the peak is only slightly affected by pressure (Fig. 1*b*). Furthermore, in these runs the reaction oc-

curred at lower temperatures with increasing pressure. These runs produced a mainly amorphous, glassy, white-gray material. Thus, the differences in the DTA patterns and the run products from the open- and closed-capsule experiments suggests that different reactions were encountered.

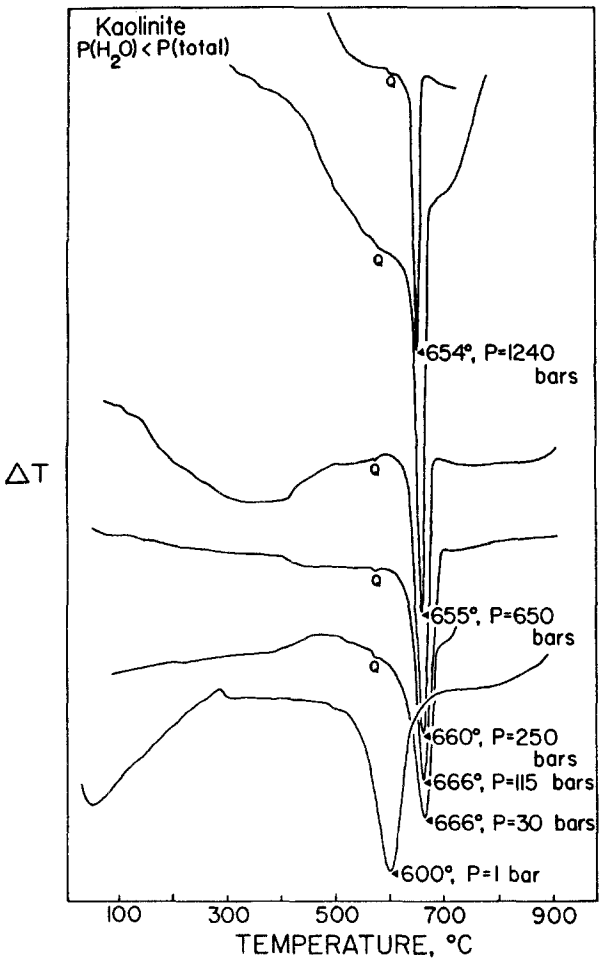


**Fig. 1a** HP-DTA patterns of kaolinite (KGa-1): Open-capsule runs; note that the peaks become very sharp at higher pressures

## Discussion

The HP-DTA data suggest the presence of several phases: kaolinite (K), metakaolinite (MK), aqueous vapor (V), and a phase with a relatively high variable vapor solubility (ML). The existence of the first three phases is well-docu-

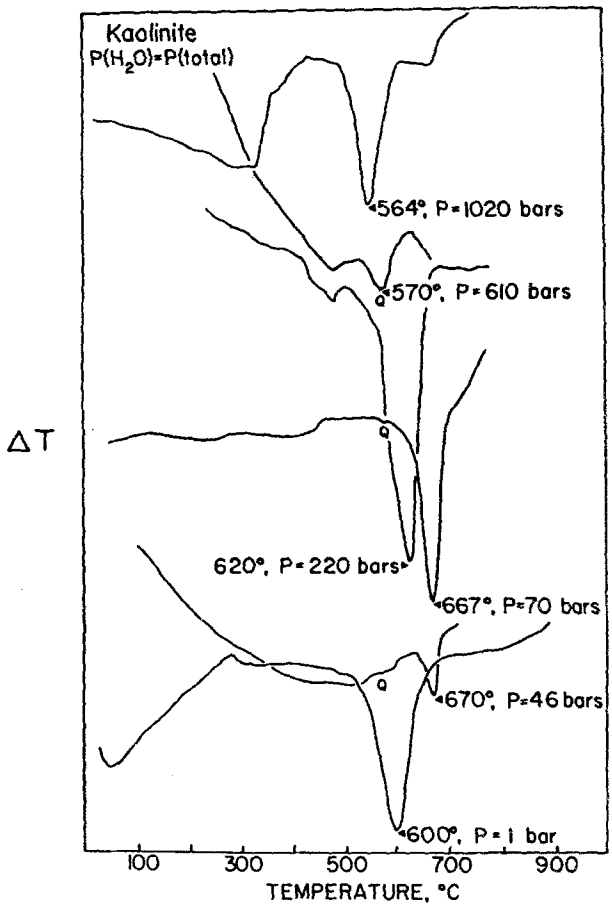


**Fig. 1b** HP-DTA patterns of kaolinite (KGa-1): Closed-capsule runs with water added. Note that the peaks are only slightly sharper at higher pressures [4]. (Q represents the low quartz-high quartz inversion, which is used for calibration purposes)

mented. The arguments for postulating the fourth phase include (*a*) the glassy nature of the run products, (*b*) the absence of a substantial amount of a crystalline phase, and (*c*) the negative slope of the reaction producing this phase, indicating a negative $\Delta V$ of reaction, probably as a consequence of the consumption of vapor in the reaction. Yeskis *et al.* [4] called this liquid-like phase 'metaliquid' (ML). The formation of a metaliquid is unusual and it may be argued that it is very similar to metakaolinite. However, a metakaolinite structure cannot accommodate large amounts of (OH). Other arguments against equating these phases are presented below.

The presence of four phases in the system metakaolinite-$H_2O$ strongly suggests that it can be considered a binary system with phase relations as shown in

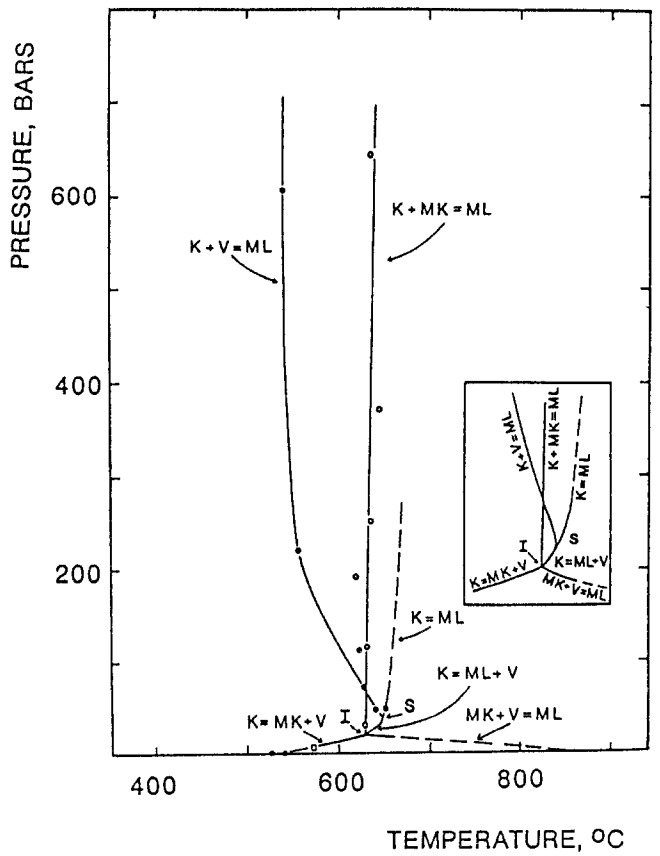


**Fig. 2** *P-T* relations in the system metakaolinite-$H_2O$. The reaction K ↔ H + M + P represents a equilibrium reaction [9]. The inset shows the reactions around the invariant points [4]. Open circles = open-capsule runs; filled circles = closed-capsule runs; open squares = data from [16]; Abbreviations: K = kaolinite, H = hydralsite, M = montmorillonite, P = pyrophyllite, MK = metakaolinite, ML = metaliquid, *V* = vapor, *I* = invariant point, *S* = singular point

Fig. 2. The relevant reactions were derived using Schreinemaker's rules (Table 2). The phase relations in this system can be understood as the intersection of the dehydroxylation reaction of kaolinite (reaction K1), which has a positive slope in *P-T* space, with melting reactions of metakaolinite or kaolinite in the presence of an aqueous vapor (reactions K2, K3, and K6). At intersection *I*, the system becomes invariant (reaction K7). Complications arise from the fact that the variable $H_2O$ content of ML requires an additional reaction (reaction K4), generating the singular point *S*. The data of Yeskis *et al.* [4] and Stone and Rowland [7] locate the invariant point at 25 ±5 bars and 625 ±5°C; the singular point is located at 40 ±10 bars and 640 ±10°C. Reaction (K5) was not observed,

presumably because at the higher temperatures most of the vapor phase was no longer present in the capsule. Reaction (K8) represents the melting of MK in the absence of vapor. It occurs at 1 atm at ~850°C [5]; it should have a steep positive slope. The general phase relations in this system are similar to that in other binary systems with hydroxyl-bearing phases, such as $CaO$-$H_2O$ [8]. It is noted that the phase relations discussed above represent metastable equilibria [9]; at ~400°C kaolinite breaks down to a hydralsite, montmorillonite, and pyrophyllite phase assemblage (Fig. 2).

**Table 2** Reactions in the system metakaolinite-$H_2O$

| | | | |
|---|---|---|---|
| K | ↔ | MK + V | (K1) |
| K | ↔ | ML + V | (K2) |
| K + V | ↔ | ML | (K3) |
| K | ↔ | ML | (K4) |
| K + MK | ↔ | ML | (K5) |
| MK + V | ↔ | ML | (K6) |
| K + MK | ↔ | ML + V | (K7) |
| MK | ↔ | ML | (K8) |

The enthalpy of dehydroxylation for kaolinite, determined from reaction (K1) and using the van't Hoff equation, is ~500 kJ/mol. This is unreasonably high, especially when compared to values of $\Delta H_{dhx}$ of ~160 kJ/mol obtained using the peak area (e.g., [10]). Johnson *et al.* [11] showed that halloysite, a hydrous form of kaolinite with an approximate chemical composition of $Al_2Si_2O_5(OH)_4 \cdot 2H_2O$ behaves similarly to kaolinite; they also obtained similar high values for $\Delta H_{dhx}$. They proposed that during dehydroxylation, the intracrystalline $f_{H_2O}$ in kaolinite and halloysite becomes significantly higher than the external fugacity of $H_2O$, which must result in a higher dehydroxylation temperature. An excess of 10-15 bars in the intracrystalline $f_{H_2O}$ would be sufficient to reconcile the differences calculated for $\Delta H_{dhx}$.

*Montmorillonite*

The dehydroxylation of SWy-1, KSWy-1, MgSWy-1, and CaSWy-1 was investigated to evaluate the effect of the interlayer cation chemistry, and to understand the mechanism of dehydroxylation [12, 13]. During this reaction the montmorillonnites lose about 4 wt% (Fig. 3). The DTG weight-loss signal is asymmetric with respect to temperature. By analogy to pyrophyllite and muscovite [14], the asymmetry is interpreted to be the result of two separate events. In SWy-1 a small event at ~650°C is followed by a major peak at ~700°C; in KSWy-1 the smaller peak is at ~630°C and the main dehydroxylation peak at

670°C. Thus, the temperatures for dehydration and dehydroxylation of KSWy-1 are lower than for SWy-1, although the onset temperature for these reactions is identical. The TG and DTG curves of the dehydroxylation for the divalent CaSWy-1 and MgSWy-1 are similar, as is the range in dehydroxylation temperatures. A major difference is that the DTG curves are more asymmetric, with the DTG curve of MgSWy-1 resolving into two peaks.

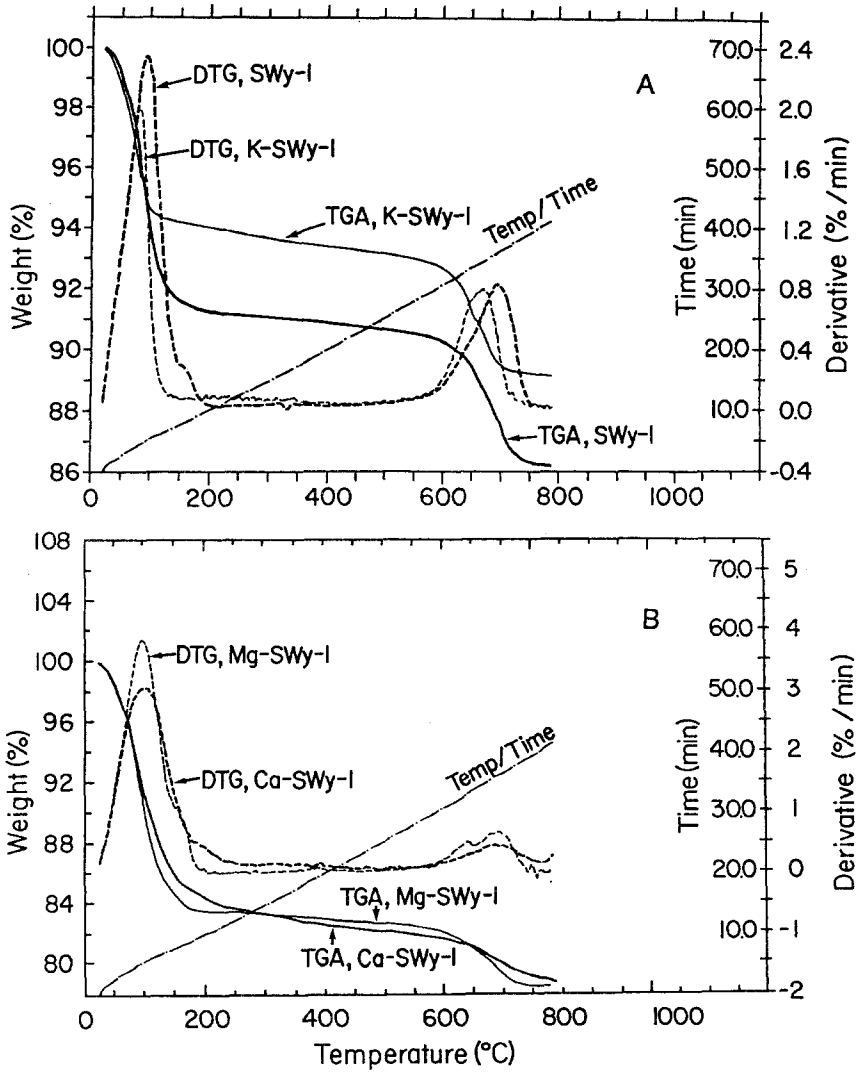


**Fig. 3** TG and DTG patterns (*A*) SWy-1 and KSWy-1, (*B*) CaSWy-1 and MgSWy-1. Temperatures for dehydration and dehydroxylation of KSWy-1 are lower than for SWy-1, although the onset temperature for these reactions is identical. Note that the interlayer water content of KSWy-1 is less than in SWy-1 [12, 13]

## HP-DTA data

HP-DTA signals of selected open- and closed-capsule analyses of these montmorillonites are shown in Figs 4 and 5 [12, 13]. A reduction in peak width in open-capsule experiments similar to that observed in kaolinite (see above) is observed in SWy-1, more so in KSWy-1, and especially in CaSWy-1. MgSWy-1 behaves differently in that two distinct dehydroxylation reactions are present, which become increasingly resolved at higher pressures, note labels at about 740°C and 790°C in Fig. 4*D*. In the closed-capsule runs no reduction in peak width was observed at higher pressures. For the various temperatures and pressures, the run products were analogous to those encountered in the kaolinite-$H_2O$ system. Thus, in the montmorillonite-$H_2O$ system, it may be assumed that different reactions occur also.

## Discussion

The thermal stability of the phases in the metakaolinite-$H_2O$ and montmorillonite dehydroxylate-$H_2O$ systems differs, but the phase relations are analogous (Fig. 6). The phases in the Na-rich, K-, and CaSWy-1 systems are montmorillonite (M), montmorillonite dehydroxylate (MD), a liquid-like phase (L) with a variable water content, and vapor (V). The existence of a montmorillonite dehydroxylate phase is based on diffraction data and by analogy to other aluminous dioctahedral 2:1 layer silicates (see [12, 13]). The reactions are listed in Table 3. Reaction (M7) represents an invariant point *I* from which four univariant reactions, (M1), (M2), (M5), and (M6) emanate. Reaction (M2) terminates in a singular point *S*, where the $H_2O$ content of the liquid becomes the same as in montmorillonite. From *S* reactions (M3) and (M4) extend to higher pressures, in which the liquid phase is richer in $H_2O$ or has the same $H_2O$ content as montmorillonite, respectively. Reaction (M6) represents the melting of MD in the presence of $H_2O$ and occurs at 1 atm at some temperature above 900°C. Reaction (M8) is the melting reaction of MD in the absence of $H_2O$. It has a positive slope and occurs at the same temperature as reaction (M6) at 1 atm.

The main difference between the *P-T* relations involving the dehydroxylation of SWy-1, KSWy-1, and CaSWy-1 is the higher temperature of reaction (M3) for KSWy-1. Clearly, KSWy-1 in the presence of water vapor is more stable with respect to the liquid phase than SWy-1 and CaSWy-1. This relationship is analogous to paragonite (Na mica) *vs.* muscovite (K mica) and is a result of the less stable configuration of a smaller Na or Ca cation in the large interlayer site (Goldschmidt's rule).

The phase relations of MgSWy-1 are more complex, although the general topology of the *P-T* diagram is similar [13]. Two reactions are observed in open-capsule experiments at pressures >1 bar but only one is encountered at 1 bar. The pronounced double dehydroxylation peak (Fig. 4*D*) can be explained by assuming two separate dehydroxylation reactions. If so, five phases must be present: montmorillonite (M), a partially dehydroxylated phase (DH1), a fully dehydroxy-

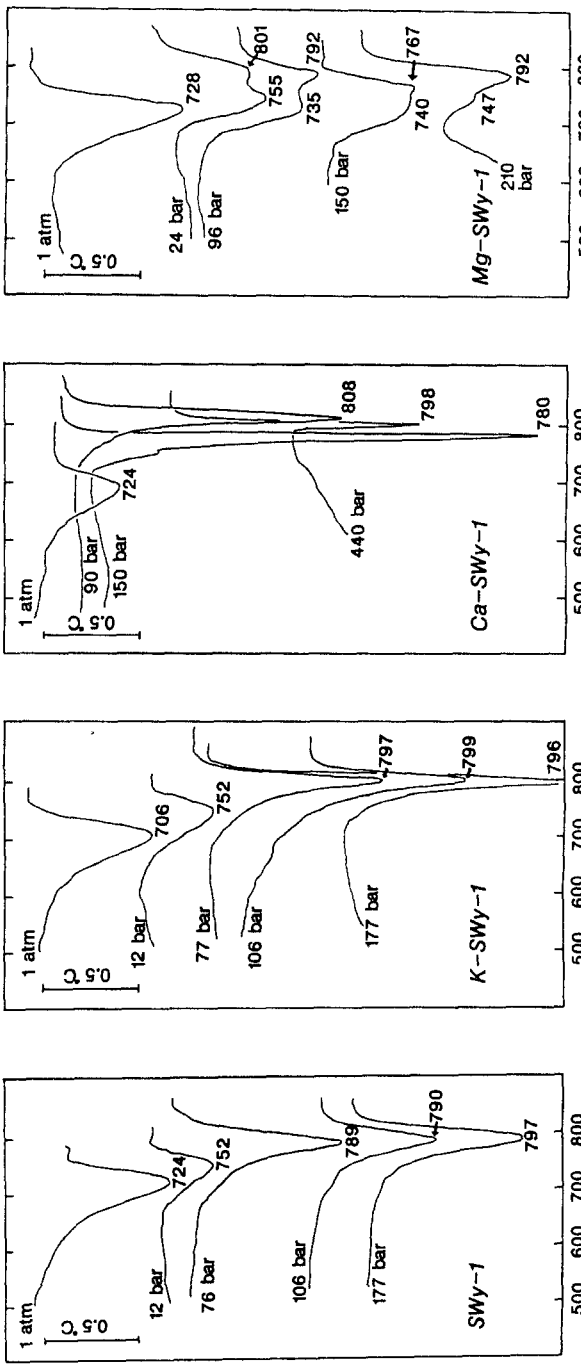


**Fig. 4** HP-DTA patterns of the dehydroxylation reaction: (*A*) SWy-1, (*B*) KSWy-1, (*C*) CaSWy-1, and (*D*) MgSWy-1, using open capsules. At higher pressures the peak width is reduced in SWy-1, more so in KSWy-1, and especially in CaSWy-1. MgSWy-1 shows two distinct dehydroxylation reactions [12, 13].

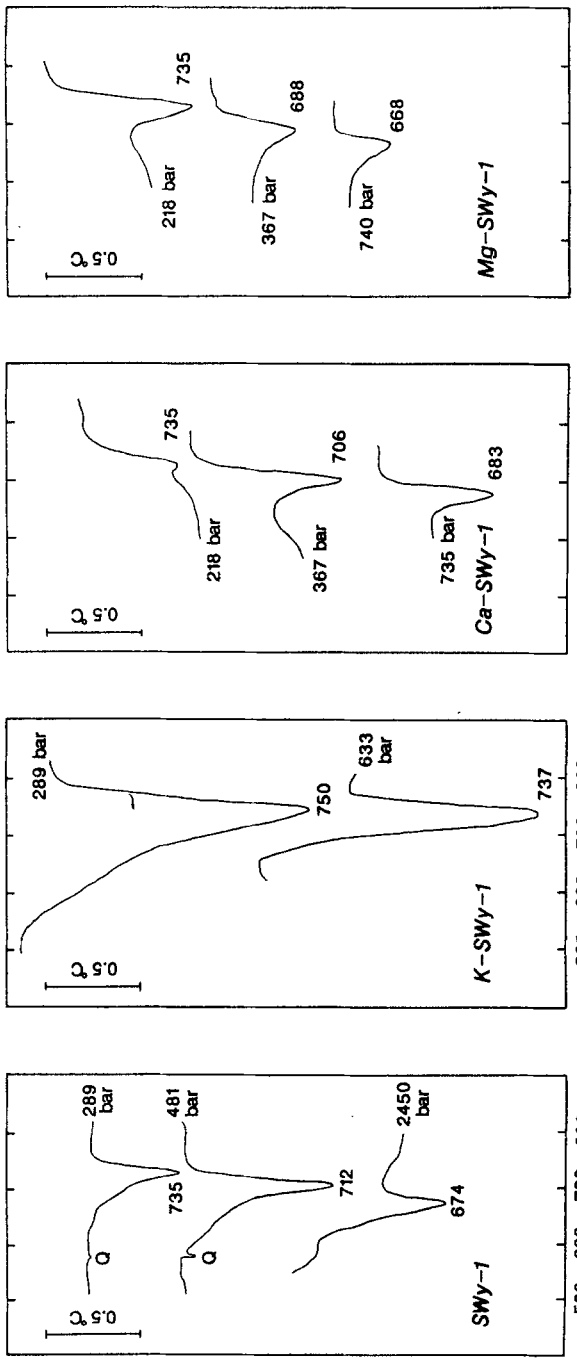


**Fig. 5** HP-DTA patterns of the dehydroxylation reaction: (*A*) SWy-1, (*B*) KSWy-1, (*C*) CaSWy-1, and (*D*) MgSWy-1, using closed capsules. The peak width is not significantly reduced at higher pressures [12]. (Q, Fig. 1)

lated phase (DH2), a liquid with a variable $H_2O$ content (L), and a vapor phase (V). The resulting *P-T* diagram is shown in Fig. 7. The additional dehydroxylated phase requires that the invariant assemblage in the Na, K, and Ca montmorillonites splits into three different invariant assemblages. The data indicate that one of these invariant points, $I_2$, lies at a very low pressure, 1.3 ±0.2 bar and at 730°C ±2°C. Thus, with a slight overpressure two dehydroxylation reactions are present (Fig. 4*D*), whereas only one dehydroxylation reaction can be observed in 1 atm experiments. For a detailed description of this system, see [13].

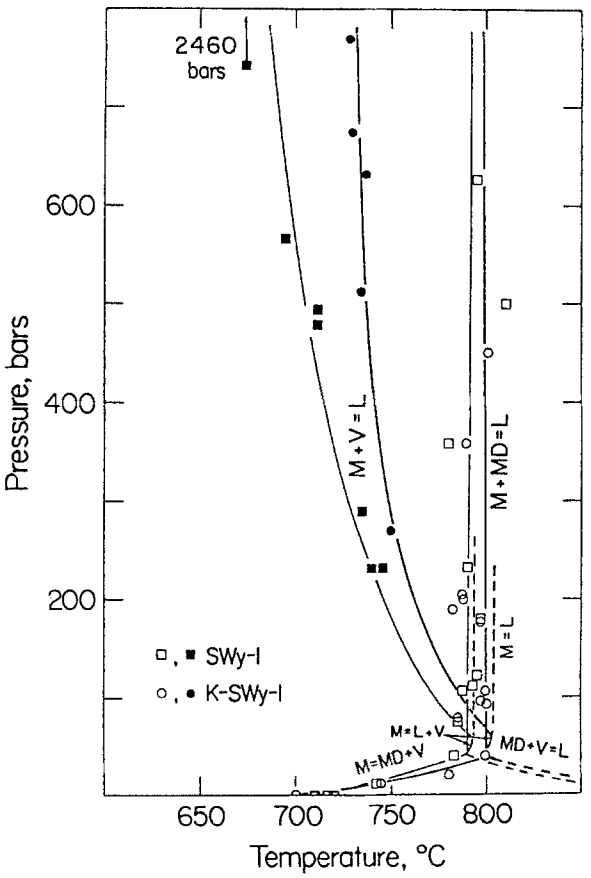


**Fig. 6a** *P-T* projections of the dehydroxylation reaction: The thin lines represent the systems (SWy-1)-$H_2O$, the heavy lines (KSWy-1)-$H_2O$ [12, 13]

The enthalpy of dehydroxylation $\Delta H_{dhx}$ of these montmorillonites, determined from reaction (M1) ranges from 260 ±50 kJ/mol for KSWy-1 to 300 ±50 kJ/mol for SWy-1 to 350 ±50 kJ/mol for CaSWy-1. For MgSWy-1 the reaction M ↔ DH2 + V has a $\Delta H_{dhx}$ = 500 ±300 kJ/mol, for M ↔ DH1 + V, $\Delta H_{dhx}$ = 600 ±100 kJ/mol,

and for DH1 ↔ DH2 + V, $\Delta H_{dhx} = 400 \pm 100$ kJ/mol. The large uncertainties relate to the difficulty in determining the slope of these reactions in *P-T* space. Furthermore, as was discussed in the section on kaolinite, possible disequilibrium because of an anomalous high intracrystallinity $f_{H_2O}$ is likely to yield enthalpy values that are too high.

## Physical dehydroxylation model

The K, Ca, and Mg-cation exchanged montmorillonites were derived from the Na-rich SWy-1. Because it may be assumed that the 2:1 layer chemistry is con-

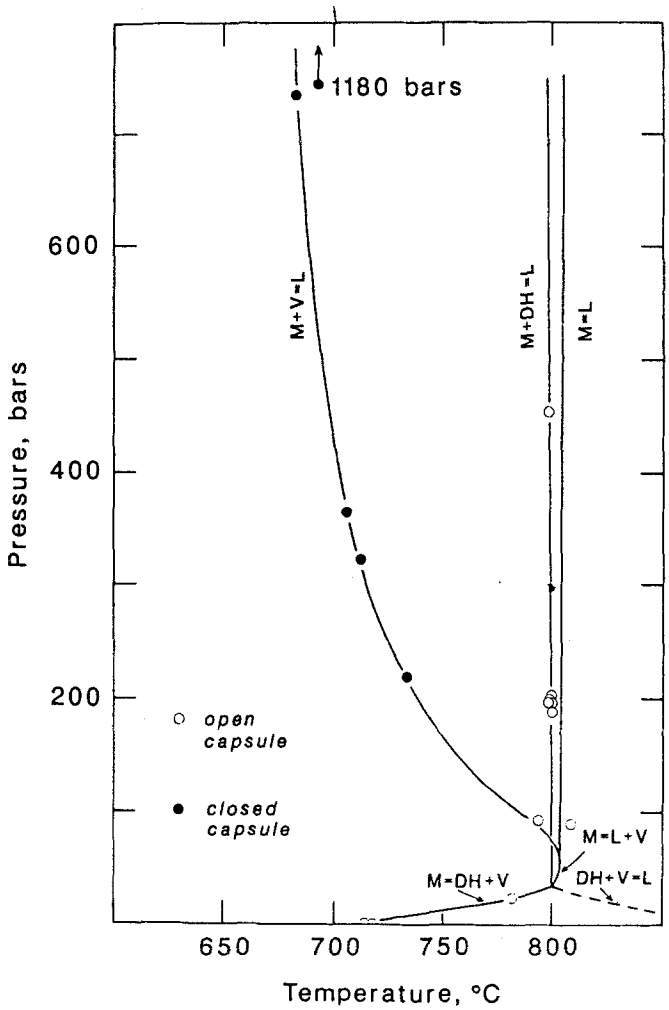


**Fig. 6b** *P-T* projections of the dehydroxylation reaction: The system (CaSWy-1)-$H_2O$. Abbreviations: M = montmorillonite, MD = montmorillonite dehydroxylate, L = liquid, for other abbreviations, Fig. 2

stant for each of these phases, the observed differences in the DTA experiments must be related to the number of interlayer sites occupied, cation size, and cation charge. It should be possible, therefore, to relate these variables to a structural model if it is known how the interlayer cation can help maintain local charge balance upon dehydroxylation.

Guggenheim *et al.* [14] suggested a model for dehydroxylation for muscovite and pyrophyllite based on single crystal X-ray studies. These phases are similar to K-montmorillonites in that this phase can be placed approximately in the chemical series of pyrophyllite-(K-montmorillonite)-muscovite. This provides a basis for a dehydroxylation model for K-montmorillonite and, because of the similarity of the structure, chemistry, and phase relations, also for Na- and Ca-exchanged montmorillonite. Modifications to this model for Mg-exchanged montmorillonites are necessary.

**Table 3** Possible reactions in the system montmorillonite dehydroxylate-$H_2O$

| | | | |
|---|---|---|---|
| M | ↔ | MD + V | (M1) |
| M | ↔ | L + V | (M2) |
| M + V | ↔ | L | (M3) |
| M | ↔ | L | (M4) |
| M + MD | ↔ | L | (M5) |
| MD + V | ↔ | L | (M6) |
| M + MD | ↔ | L + V | (M7) |
| MD | ↔ | L | (M8) |

For muscovite and pyrophyllite, Guggenheim *et al.* [14] suggested a model for dehydroxylation in which the strength of the Al–OH bond is greatly affected by the coordination number of *neighboring* cations. Developed from first principles by using Pauling bond-strength summation calculations, it may also explain the shape of peaks derived from thermo-analytical experiments.

The model, illustrated by using pyrophyllite, is presented in Fig. 8. Pauling's electrostatic valency principle states that, in a stable structure, the total strength of the bonds that reach an anion from all neighboring cations is equal to the formal charge of the anion, but opposite in sign. Figure 8A shows Pauling bond-strength summations for selected oxygen atoms for pyrophyllite; Figure 8B shows similar summations in the pyrophyllite dehydroxylate structure, the high temperature phase that develops topotactically from pyrophyllite. Unlike pyrophyllite where all oxygens are charge saturated at 2.0 electrostatic valency units (esu), the dehydroxylate consists of Al polyhedra with one charge-undersaturated oxygen (at 1.2 esu) and the remaining oxygens charge-oversaturated (at 2.2 esu each). In order to compensate for this charge imbalance, the Al cation moves closer to the undersaturated oxygen and away from the oversaturated

oxygens. This qualitative prediction of changes in bond distance is important because bond distance is directly correlated to bond strength, with smaller distances corresponding to stronger bonds.

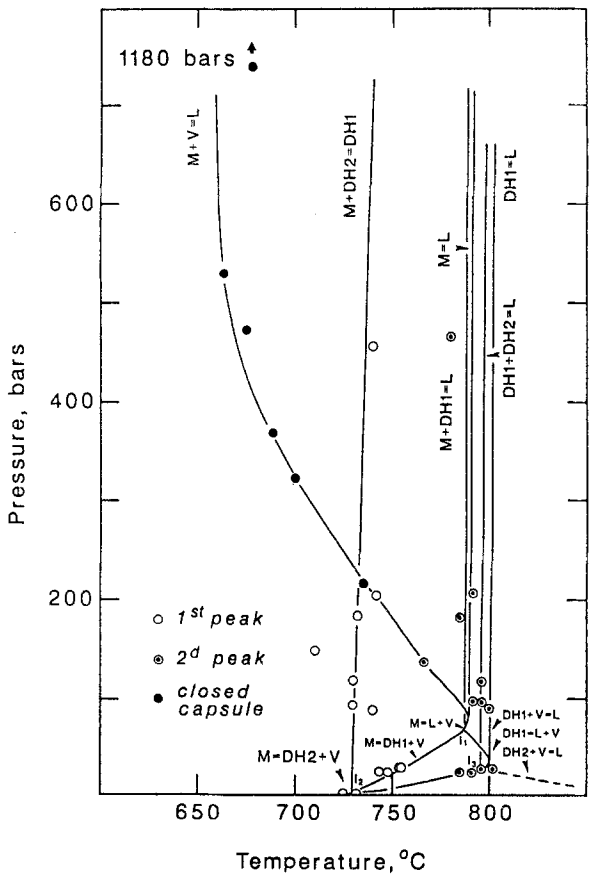


**Fig. 7** *P-T* projections of the dehydroxylation reactions in the system (MgSWy-1)-$H_2O$ [13]. Abbreviations: DH1 = partial dehydroxylated montmorillonite, DH2 montmorillonite dehydroxylate, for other abbreviations, Figs 2, 6

Similar summation calculations may be made for a partially dehydroxylated pyrophyllite structure (Fig. 8C). Note that some Al cations are in five-fold coordination as in the dehydroxylate structure, and a pair are in six-fold coordination as in pyrophyllite. Calculated summation values show asymmetric distributions for each six-fold coordinated Al cation. Therefore, that cation moves away from the side of the octahedron with oversaturated oxygens toward the saturated oxygen of the hydroxyl group. Hydroxyl protons can readjust their positions to polarize further the hydroxyl oxygen, thereby making a closer approach of the Al cation to the hydroxyl more stable. The increased attraction between the Al and

its coordinating hydroxyl is a consequence of the neighboring five-fold coordinated site.

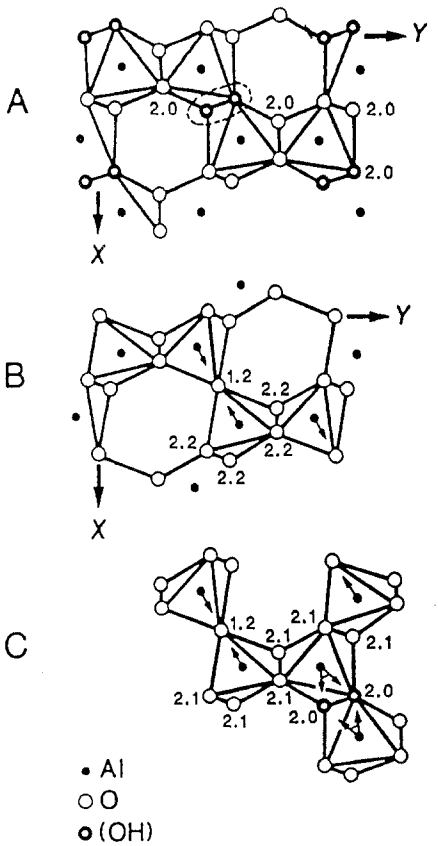


**Fig. 8** Al polyhedra of pyrophyllite (*A*), pyrophyllite dehydroxylate (*B*), and pyrophyllite in transition (*C*) due to thermal stress. Numbers associated with oxygen atoms refer to Pauling bond-strength summations (refer to text). Note that the dashed oval in (*A*) refers to the pair of hydroxyls involved in water loss; compare to (*B*) and (*C*). Arrows associated with Al cations indicate predicted direction of movement as determined from the summation calculations (from [18] as modified from [14])

The model predicts, therefore, that partial dehydroxylation occurs at lower temperatures where Al neighbors to the pair of Al octahedra in question are in six-fold coordination. However, after partial dehydroxylation, remaining hydroxyls are more tightly held where Al neighbors are five-fold coordinated. A bimodal distribution of hydroxyl loss is anticipated (Fig. 9). However, both five-fold *and* six-fold Al neighbors are possible, and such arrangements produce broadening of the thermal peaks. In addition, because hydroxyl (or $H_2O$) diffusion occurs

through the interlayer (see [14] for additional details), interlayer site occupancy may also affect the thermal peak shape and the temperature of dehydroxylation.

Mg-exchanged montmorillonite differs from the other forms because of the small size of Mg and its ability to migrate into the silicate ring of the 2:1 layer [15]. Above about 1.5 bar, partial dehydroxylation in MgSWy-1 occurs at lower temperatures than either the Na, Ca, or K forms. Thus, Mg initially destabilizes the fully hydroxylated 2:1 layer.

With the first loss of OH, Mg enters the silicate ring to neutralize the undersaturated residual oxygen. The small size of Mg allows it to reach an equilibrium

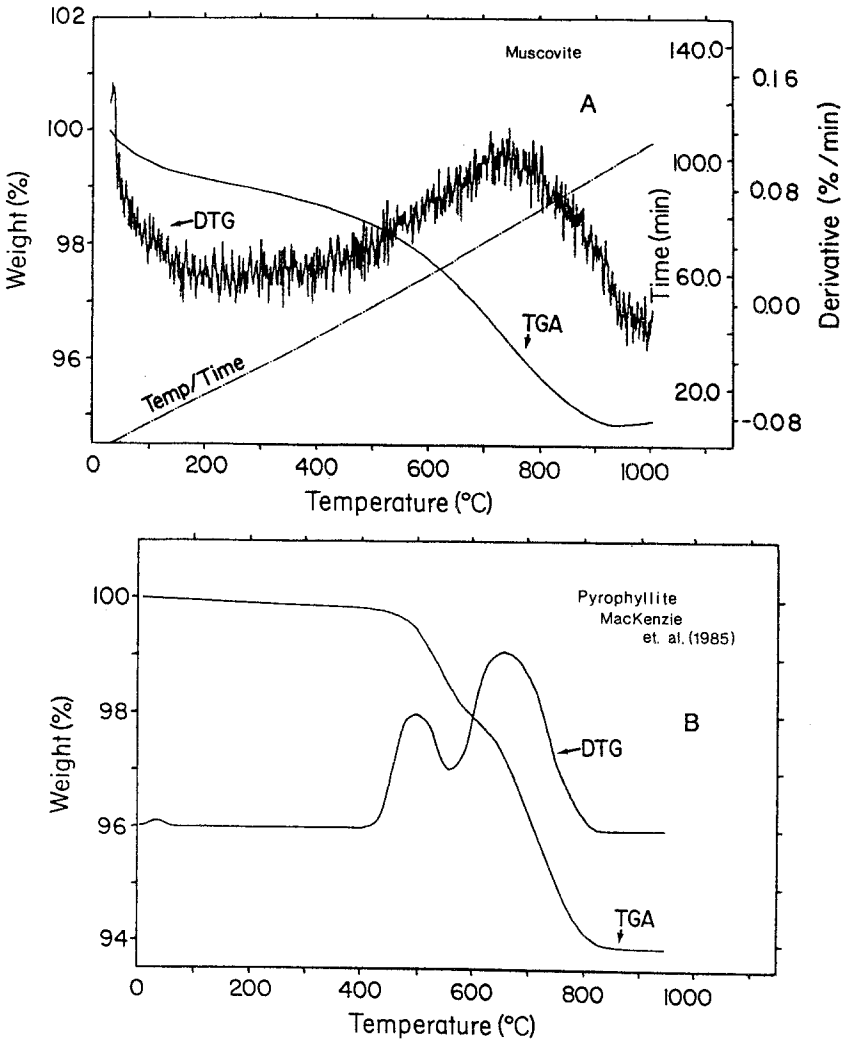


**Fig. 9** TG and DTG diagrams for muscovite (*A*) and Pyrophyllite (*B*) (from [14])

distance to the residual oxygen, and thus stabilizes the structure around the residual oxygen. Because about a third of the available interlayer sites are filled by Mg in the low temperature form, the process can continue until each Mg is associated with a residual oxygen as dehydroxylation proceeds. The DHl phase, therefore, is a partially dehydroxylated phase stabilized by Mg cations associated with residual oxygens.

With increasing temperature, the DH2 phase forms by a second set of dehydroxylation reactions which produces a fully dehydroxylated phase. Because the DTA peak involved in the formation of DH2 is at a similar temperature as the single peak representing dehydroxylation of SWy-1, KSWy-1, and CaSWy-1, it suggests that the DH1 phase is nearly equivalent in thermal stability to the hydrated forms (M) involving Na, K, and Ca. This accounts for the similarity in slopes and disposition between M $\leftrightarrow$ DH + V for the Na, K, and Ca montmorillonite phases and DH1 $\leftrightarrow$ DH2 + V for Mg montmorillonite in the phase diagrams. At higher pressures, the dehydroxylation reactions are replaced by melting reactions and the DTA peaks become considerably sharper. Further details are given in [13].

### *Chlorite*

An indication of the importance of water fugacity to the thermal response of the chlorites was given by Stone and Weiss [16]. They used a 'dynamic gas method' in which steam was forced through the chlorite samples during the DTA experiment. At pressures of up to three atmospheres, they observed remarkable changes in the characteristics of the DTA patterns: 1) an exothermic peak observed near vacuum conditions is suppressed at 1 atm, 2) a single endotherm appeared to be replaced by two or more peaks at higher pressures, and 3) another endotherm appears to diminish at 3 atm relative to a 1 atm run. The results are difficult to evaluate because samples contained impurity phases, both $Fe^{2+}$ and $Fe^{3+}$ were present in the chlorites studied, sample particle size was large (<0.5 mm) to facilitate the flow of steam, and each sample had an asymmetric distribution of iron between the two octahedral sheets with more of the iron located in the brucite-like interlayer than in the 2:1 layer. Nonetheless, the effect of the fugacity of water is pronounced and additional studies are needed to understand fully how pressure and water fugacity affect chlorite decomposition.

## Conclusions

The previous sections illustrate the diversity of $H_2O$-loss reactions in layer silicates with respect to pressure and temperature. The understanding of important elements of structure of these minerals was strongly enhanced by the results of these studies. As such, HP-DTA provides an important method for the charac-

terization and understanding of materials. Combined with the development of a simplified HP-DTA apparatus, it can be expected that HP-DTA will become an important analytical and research tool.

An obvious future use of HP-DTA in clay mineral studies will be in identifying phases or mixes of phases. Depending on the phase relations of these materials, one or two pressures may be chosen so that the temperatures of the thermal reaction event are clearly separated for the different phases of the mixture. Other pressures may be chosen to confirm the initial identification. Chemical pre-treatments can be used to enhance the results further. For example, calcium-exchanged montmorillonites produce extremely sharp peaks in open capsules above 45 bars, as does kaolinite. Montmorillonite-kaolinite mixtures, therefore, can be successfully analyzed quantitatively at elevated pressures (e.g., [17]). Initial results suggest that relatively small differences in particle size and crystallinity do not significantly affect the results at high pressure. In contrast, X-ray diffraction techniques are severely affected by these properties.

Early workers using traditional DTA methods recognized the potential use of the method as a tool to measure clay fractions quantitatively. These expectations were not realized because of broad, poorly-defined peaks, unpredictable results originating from overpressure development, and non-reproducible sample geometry. The use of small sample sizes, numerical analysis by direct computer linkage to the HP-DTA system, reproducible sample geometry, and a better understanding and assessment of environmental conditions in the system should allow the development of a precise quantitative tool for clay mineral analysis by HP-DTA.

* * *

Support for this work was provided by the Petroleum Research Fund of the American Chemical Society under grants #21974-AC8-C and 20016-AC2, and the National Science Foundation under grants #EAR-9003688 and EAR-8816898.

## References

1 S. Guggenheim and A. F. Koster van Groos, J. Thermal Anal., 38 (1992) 1701.
2 A. F. Koster van Groos and S. Guggenheim, 'Thermal Analysis in Clay Science' J. W. Stucki, D. Bish and F. A. Mumpton, eds., Clay Minerals Society, Boulder, 1990.
3 H. van Olphen and J. J. Fripiat, Eds., Data Handbook for Clay Materials and other Non-metallic Minerals, Pergamon Press, Oxford 1979.
4 D. Yeskis, A. F. Koster van Groos, and S. Guggenheim, Amer. Mineral., 70 (1985) 159.
5 R. Roy, D. M. Roy, and E. E. Francis, Amer. Ceram. Soc. Jour., 38 (1958) 198.
6 G. W. Brindley, and M. Nakahira, J. Amer. Ceram. Soc., 42 (1959) 311.
7 R. L. Stone and R. A. Rowland, Clays Clay Minerals, 3 (1954) 103.
8 P. J. Wyllie, J. Am. Ceram. Soc., 42 (1959) 448.
9 R. Roy and E. F. Osborn, Amer. Mineral., 39 (1954) 853.
10 J. N. Weber and R. Roy, Amer. Ceram. Soc. Jour., 48 (1965) 309.

11 S. L. Johnson, S. Guggenheim and A. F. Koster van Groos, Clays Clay Mineral., 38 (1990) 477.
12 A. F. Koster van Groos and S. Guggenheim, Amer. Mineral., 72 (1987) 1170.
13 A. F. Koster van Groos and S. Guggenheim, Amer. Mineral., 74 (1989) 627.
14 S. Guggenheim, Y.-H. Chang and A. F. Koster van Groos, Amer. Mineral., 72 (1987) 537.
15 R. Tettenhorst, Amer. Mineral., 47 (1962) 769.
16 R. L. Stone and E. J. Weiss, Clay Minerals Bull., 3 (1956) 214.
17 A. F. Koster van Groos, Sci. Geol. Mem., 89 (1990) 123.
18 B. W. Evans and S. Guggenheim, 'Hydrous phyllosilicates and other non-mica layer silicates' S. W. Bailey, ed., Mineralogical Society of America, 1988,p. 225.

**Zusammenfassung** — Ergebnisse der Hochdruck-DTA werden zur Beschreibung der Dehydroxylierungsreaktionen der Tonmaterialien von Kaolinit, Na-reichem Montmorillonit und K-, Ca- und Mg-ausgetauschtem Montmorillonit verwendet. Verschlossene Kapseln können verwendet werden, um Fluids zu enthalten und es ist möglich, die Rolle des Wassers in diesen Reaktionen aufzuzeigen. Weiterhin werden Strukturinformationen zusammen mit DTA-Daten verwendet, um atomistische Modelle zum Verständnis dieser Prozesse zu entwickeln.